

GREISEN AND POST-GREISEN ALTERATION IN THE SÃO VICENTE DE PEREIRA KAOLINITE DEPOSIT, PORTUGAL

JULIU BOBOS¹ AND CELSO GOMES

Departamento de Geociencias, Universidade de Aveiro, Aveiro 3810, Portugal

ABSTRACT

The São Vicente de Pereira kaolinite deposit, located at the northwestern border of the Ossa Morena zone, in Portugal, is the site of important hydrothermal alteration, developed at the expense of migmatitic rocks and related to a system of Hercynian polyphase deformation and shear zones. Two stages of hydrothermal alteration are evident: 1) greisen-type alteration is represented by quartz + muscovite containing F and Cl, and by quartz + tourmaline; 2) post-greisen alteration and advanced argillic alteration led to the formation of well-ordered or poorly ordered kaolinite. The quartz + muscovite assemblage was investigated by XRD and electron-microprobe analyses. The mica shows intermediate characteristics between muscovite and lepidolite. It has a relatively low content of Si (3.10–3.20 *apfu*), a high proportion of ^{VI}Al, a very low Fe content, and an absence of Mg. Quartz–tourmaline-rich greisen occurs in veinlets that cross-cut migmatites showing advanced argillic alteration. Two generations of tourmaline having different morphologies and different Fe contents can be identified. Well-ordered kaolinite formed at the expense of muscovite exhibits a “booklet” morphology, as revealed by SEM and TEM observations. The hydration of well-ordered kaolinite led to halloysite-7Å. Results of O and H isotopic analyses attest to the formation of kaolinite from metamorphic pore-fluid.

Keywords: greisen, post-greisen alteration, kaolinite, halloysite-7Å, X-ray diffraction, electron microprobe, electron microscopy, isotopic ratios, oxygen, hydrogen, Portugal.

SOMMAIRE

Le gisement de kaolinite de São Vicente de Pereira, situé à la frontière nord-ouest de la zone d'Ossa Morena, au Portugal, est le site d'une importante altération hydrothermale, développée aux dépens de roches migmatitiques, et liée à un système de déformation polyphasée et de zones de cisaillement d'âge hercynien. Deux stades d'altération sont évidents: 1) altération de type greisen, que représentent les associations quartz + muscovite contenant F et Cl, et quartz + tourmaline; 2) altération postérieure au développement de greisen et altération argillique avancée, qui ont mené à la formation de kaolinite plus ou moins bien ordonnée. L'assemblage quartz + muscovite a été étudiée par diffraction X et analysée avec une microsonde électronique. Le mica possède une composition intermédiaire entre la muscovite et la lépidolite. Il a une teneur relativement faible en Si (3.10–3.20 *apfu*), une proportion élevée d'aluminium hexa-coordonné, une très faible teneur en Fe, et une absence de Mg. Les greisens à quartz–tourmaline occupent des veines qui recoupent les roches migmatitiques affectées par l'altération argillique avancée. On distingue deux générations de tourmaline, ayant des morphologies et des teneurs en Fe différentes. La kaolinite bien ordonnée se présente en empilements de feuillets formés aux dépens de la muscovite, comme le révèle les observations en microscopie électronique par transmission. L'hydratation de la kaolinite bien ordonnée a donné la halloysite-7Å. Les résultats d'analyses isotopiques de l'oxygène et de l'hydrogène sont conformes avec un mode de formation à partir d'une phase fluide métamorphique.

(Traduit par la Rédaction)

Mots-clés: greisen, altération post-greisen, kaolinite, halloysite-7Å, diffraction X, microsonde électronique, microscopie électronique, rapports isotopiques, oxygène, hydrogène, Portugal.

INTRODUCTION

Greisenization takes place as a result of the interaction of a granitic host-rock with a fluorine-bearing, acid magmatic fluid of generally low salinity at temperatures between 250° and 450°C (e.g., Barnes 1979, Štemprok

1987, Pirajno 1992). In most cases, the granitic rocks that host greisen occur along deep crustal faults and are associated with cupola-like structures, where fluids are concentrated during crystallization. The greisen system evolves by a decrease in the ratio alkali/H⁺, resulting in the destabilization of primary minerals and their replacement with a quartz + “muscovite” assemblage.

¹ E-mail address: juliu@geo.ua.pt

In Portugal, most occurrences of greisen (Panasqueira, Gerês, Trás-os-Montes) are related to Hercynian Sn–W mineral deposits. The São Vicente de Pereira kaolinite deposit hosts an exogreisen composed of quartz–muscovite and quartz–tourmaline assemblages (Gomes *et al.* 1990). Our aim here is to describe the unmineralized exogreisen chemically and mineralogically and to show the structural transition from greisen to post-greisen alteration. Pollard (1983) showed a sequence of late- to postmagmatic processes leading to greisenization, which were taken into account in our study.

The São Vicente de Pereira deposit is one of the main sources of kaolinite used by famous porcelain factory of Vista Alegre. Kaolinite is exploited in the quarries, being excavated to depths of 10–15 meters. The entire region is highly cultivated or forested, with few outcrops.

GEOLOGICAL BACKGROUND

The northwestern border of the Ossa Morena zone consists of metamorphic rocks: micaceous schist, gneiss, migmatite gneiss and tonalite gneiss of Middle Proterozoic age, and porphyroblast-bearing schist, chlorite–muscovite schist, amphibolite, felsic metavolcanic rocks of Late Proterozoic age (geological map of Portugal, scale 1:500,000, 1992). Four lithostratigraphic units have been defined by Ribeiro *et al.* (1995) and Chaminé *et al.* (1995) in the northwestern border of the Ossa Morena zone: these are the São João-de-Ver, Arada, Espinho and Lourosa units (Fig. 1). Chaminé *et al.* (1995) divided the Lourosa unit in two members: lower (migmatite, orthogneiss) and upper (micaceous schist with garnet).

The tectonic evolution of the region is represented by four phases (D_1 , D_2 , D_3 , D_4) of Hercynian deformation (Aguado 1992). However, other authors recognize only three phases (Ribeiro *et al.* 1995).

The Oliveira de Azemeis granitic massif, contemporary with post- D_2 or pre- D_3 deformation (Aguado 1992), outcrops to the south of the northwestern border of the Ossa Morena zone. To northeast and north of the São Vicente de Pereira area, sparsely distributed small bodies of two-mica granite (*e.g.*, the Mosteiro granite) cross-cut the migmatized central part of the D_3 antiform (Ribeiro *et al.* 1995). According to Aguado (1992), they were emplaced during a late phase of the D_3 tectonic event.

The migmatite complex hosts greisen and post-greisen alteration. As a rule, between micaceous schist and migmatite, a diffuse contact can be observed showing advanced argillic alteration in the São Vicente de Pereira area. Migmatization was considered by Aguado *et al.* (1993) to be contemporary with D_3 deformation (approximately 320 Ma, Upper Paleozoic). Advanced argillic alteration affected the migmatite, which is cross-cut by tourmaline + quartz veins and quartz veins with

a general attitude N95°E. Silicification and tourmalinization are two postmagmatic processes identified in the São Vicente de Pereira area, as well as to the north of this area. The quartz–tourmaline-bearing assemblage occurs as veins 10 to 15 cm wide and veinlets of disseminated tourmaline in the zone of advanced argillic alteration. Tourmaline + quartz veins are accompanied in their external part by large flakes of muscovite and by K-feldspar, both with a high degree of alteration.

Also, zones of quartz + muscovite greisen occur in the heavily altered migmatite complex. Small flakes of muscovite are recognized macroscopically by their light yellowish green color, exfoliated and transformed to kaolinite.

Two stages of alteration were described by Bobos & Gomes (1996) in the São Vicente de Pereira kaolinite deposit: hydrothermal and supergene. Hydrothermal alteration is characterized by a greisen-type alteration, represented by quartz + muscovite containing F and Cl, and quartz + tourmaline, whereas post-greisen-type alteration is represented by well-ordered kaolinite and the assemblage kaolinite + illite. The weathering stage is expressed by transformation of kaolinite to halloysite-7Å.

Hydrothermal activity in the deposit is related to a system of deformation that includes faults, fractures and shear zones. Hydrothermal fluids are associated genetically and spatially with felsic intrusive bodies and with fluids of metamorphic origin (Bobos & Gomes 1996).

The shear zone is characterized by the development of an intense foliation in migmatite. The largest shear zone is coincident with the elongate system of alteration hosting the advanced argillic and post-greisen alteration. The migmatite zone can be considered as an external marker of a shear zone with continuous offsetting along a discrete surface. The migmatite complex and, in particular, the shear zone, show evidence of the passage of large volumes of fluid. Introduction of vast quantities of H₂O into major structural breaks is a major cause for the widespread alteration on a regional scale. The metasomatic fluid in the shear zone may have been derived from the migmatization process.

MATERIALS AND METHODS

Samples were taken along two horizontal profiles in the São Vicente de Pereira area. Tourmaline and muscovite from the quartz–tourmaline and quartz–muscovite assemblages were separated. Clay fractions less than 2 µm were separated by sedimentation.

All samples were analyzed by X-ray diffraction (XRD) using a Philips PW-1710 diffractometer (40 kV, 20 mA, CuK α radiation), with a scanning speed of 1° 2 θ per minute.

Chemical analyses of muscovite and tourmaline were performed with a JEOL JSM-35 electron microscope equipped with an energy-dispersion spectrometer (EDAX) facility. The accelerating voltage was 15 kV,

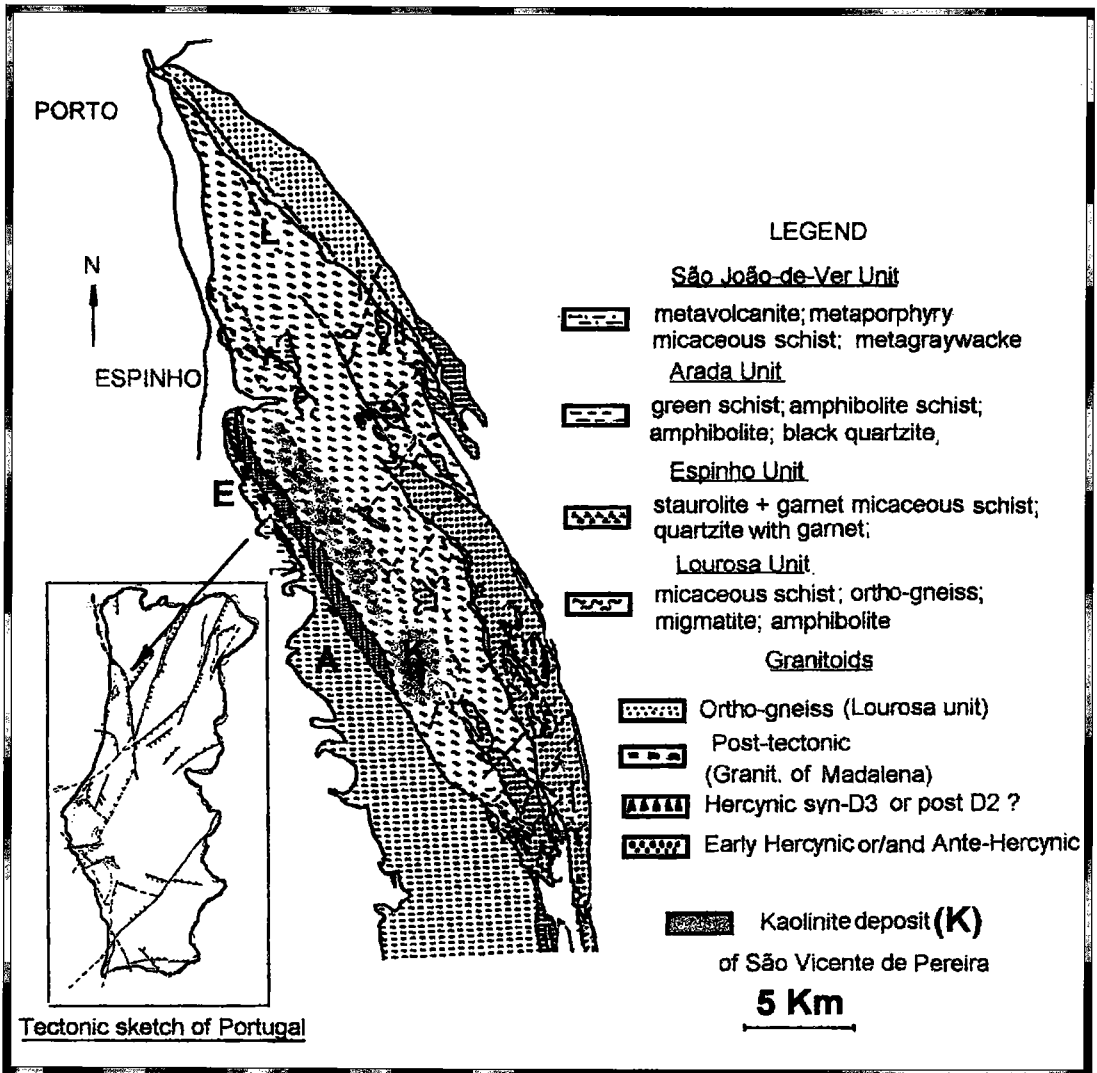


FIG. 1. Geological sketch of the northwestern sector of Ossa Morena zone (after Chaminé *et al.* 1995). A: Arada Unit, E: Espinho Unit, L: Lourosa Unit. The kaolinite deposit (K) of São Vicente de Pereira is located in the Lourosa unit.

and the intensity data were corrected with a ZAF program. The Li content of mica was determined by atomic absorption spectrometry using a GBC 906–908 type of spectrometer. The concentrations of trace elements in mica and the chemical composition of kaolinite were determined using X-ray fluorescence (XRF), with the fused disk method.

The less than 2 μm fractions containing kaolinite were investigated by transmission electron microscopy (TEM) using a Hitachi H-9000 electron microscope, operated at 80 kV. The clay fraction was dispersed using

an ultrasonic bath. From the dispersion, after convenient dilution, one drop of the suspension was spread over carbon microgrids.

For SEM observations, a few plates of muscovite were crushed into several fine grains and cleaned ultrasonically afterward. Samples of muscovite and tourmaline were mounted on a carbon holder.

Oxygen and deuterium isotope analyses on kaolinite were performed according to Girard & Fouillac (1995) and the methodology used in the Centre de Géochimie de la Surface in Strasbourg (France).

GREISEN ALTERATION

Quartz-muscovite greisen

Quartz-muscovite greisen occurs marginally in the quartz veins, and the flakes of muscovite range from 32 to 63 μm in size. XRD data reveal intermediate structural characteristics between lepidolite and muscovite. These two phases were distinguished, according to the position of the 060 reflection: 1.525 \AA for lepidolite and 1.495 \AA for muscovite (Brindley & Brown 1980). SEM analyses reveal structural arrangements expressed by crenulations and microfolds (Fig. 2), which indicate that mica grains were affected by at least one of the major regional tectonic deformations (D_3 or D_4). Exfoliation of the mica grains was documented in SEM investigations.

Electron-microprobe analyses (Table 1) of the light yellowish green mica grains reveal Si contents ranging from 3.11 to 3.33 atoms per formula unit (*apfu*) and occupancies of the octahedral sites close to 2.00 *apfu* on the basis of 11 atoms of oxygen. A few muscovite specimens show a low K content and a greater-than-normal amount of $^{\text{VI}}\text{Al}$, representative of transition stages from muscovite to kaolinite, and perhaps mixtures. The chemical data are in agreement with the SEM evidence of pseudomorphs of illite and kaolinite after muscovite. In the diagram M^{2+} ($= \text{Fe}^{2+} + \text{Mn} + \text{Mg}$) - Al - Si (Fig. 3), the data points are located close to the muscovite field. The muscovite specimens are rich in $^{\text{IV}}\text{Al}$ and $^{\text{VI}}\text{Al}$ and poor in Si, Ti, Fe_{tot} and Mg, indicative of secondary muscovite, probably formed from the alteration of plagioclase. The lithium content is low,

ranging between 22 and 17 ppm in muscovite and between 6 and 8 ppm in muscovite transformed to kaolinite. The lithium presumably is octahedrally coordinated. The fluorine content was only qualitatively established. Trace elements in the muscovite (Table 2) show a progressively increase of Rb, Sn, Y, Nb, Cu, Pb, and Zn with increasing degree of alteration.

TABLE 1. CHEMICAL COMPOSITIONS OF MUSCOVITE* FROM EXOGREISEN ALTERATION

Samples	1	2	3	4	5	6	7	8	9
<i>n</i> *	4	3	6	5	4	4	5	4	4
SiO ₂	50.11	50.03	49.76	50.84	48.96	49.92	50.29	52.00	50.95
Al ₂ O ₃	39.69	40.02	37.10	38.67	36.99	38.08	37.81	38.19	33.34
FeO	0.12	0.05	1.23	1.79	0.86	0.53	1.04	0.89	1.11
CaO	0.03	0.00	0.00	0.00	0.00	0.00	0.00	0.00	0.14
MgO	0.00	0.00	0.00	0.00	0.00	0.00	0.00	0.00	0.00
Na ₂ O	0.30	0.22	0.25	0.35	0.00	0.15	0.15	0.03	0.90
K ₂ O	9.57	8.85	11.65	8.21	13.09	11.24	10.51	8.89	8.98
P ₂ O ₅	0.14	0.44	0.00	0.00	0.00	0.00	0.00	0.00	0.00
SO ₃	0.00	0.00	0.01	0.00	0.00	0.00	0.00	0.00	0.00
Cl	0.04	0.00	0.00	0.10	0.06	0.08	0.08	0.08	0.04
Total	100.00	100.00	100.00	100.00	100.00	100.00	100.00	100.00	100.00
number of cations (<i>apfu</i>) calculated on the basis of 11 atoms of oxygen									
Si	3.12	3.11	3.15	3.18	3.12	3.14	3.15	3.21	3.33
$^{\text{IV}}\text{Al}$	0.88	0.89	0.85	0.82	0.88	0.86	0.85	0.79	0.67
$^{\text{VI}}\text{Al}$	2.01	2.05	1.92	2.04	1.91	1.96	1.95	2.00	1.89
Fe	0.00	0.00	0.07	0.00	0.05	0.03	0.05	0.01	0.06
Ca	0.00	0.00	0.00	0.00	0.00	0.00	0.00	0.00	0.01
Mg	0.00	0.00	0.00	0.00	0.00	0.00	0.00	0.00	0.00
Na	0.04	0.00	0.07	0.04	0.00	0.02	0.03	0.00	0.11
K	0.76	0.70	0.94	0.66	1.07	0.91	0.84	0.70	0.75

* Expressed in weight % on an anhydrous basis. *n*: Number of analyses carried out.

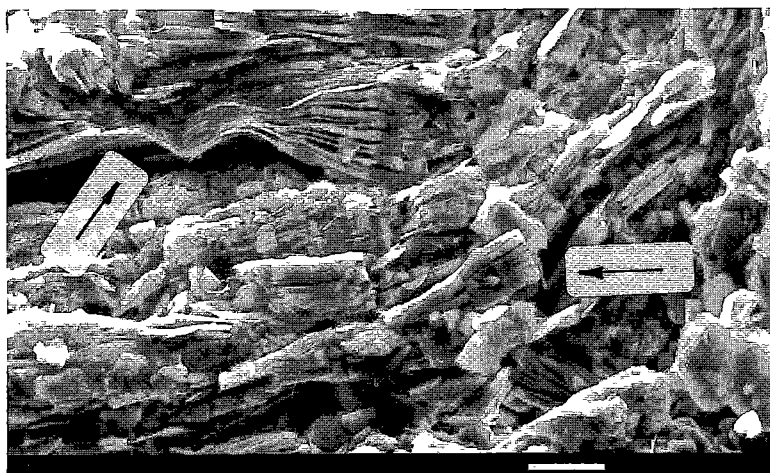


FIG. 2. SEM image of muscovite from the greisen showing exfoliation and microfolds (arrows). Scale bar: 10 μm .

Neiva *et al.* (1990) showed that hydrothermal alteration associated with the granitic bodies from Portugal leads to a general decrease in Fe, Mg, Ca, Cr, Sr, and Ba and to an increase in H₂O, Rb, F, Sn, Nb, Y, V, and Ni. In general, Zr remains constant or decreases. Also, Neiva & Campos (1993) showed that in recrystallized muscovite, the contents of Zn, F, Sn, Li, Y and Rb are higher than in muscovite from fresh granites.

Quartz-tourmaline greisen

Quartz-tourmaline veinlets are widespread throughout the kaolinite deposit. The tourmaline crystals analyzed by SEM exhibit two distinctive morphologies: acicular, and polygonal with an incipient zonation. Tourmaline (Fig. 4) is characteristically very fine grained, generally less than 20 μm . Acicular tourmaline is considered as a later generation and corresponds to the hydrothermal tourmaline of London & Manning (1995). Chemical analyses reveal two distinctive types of tourmaline (Table 3). Structural formulae were calculated on the basis of 24.5 atoms of oxygen per formula unit. Boron was treated as obeying stoichiometry. A type of tourmaline enriched in Fe and another type with low Fe content were found. That with the higher proportion of Fe presumably indicates a higher oxidation state (samples 1 and 1a). These two types of tourmaline are compared in terms of Fe *versus* Mg (Fig. 5). Substitution toward schorl-dravite is shown in a plot of Fe *versus* Mg for tourmaline having a polygonal habit. In the case of the acicular tourmaline, it has a schorl composition.

LATE HYDROTHERMAL ALTERATION SURROUNDING QUARTZ-TOURMALINE VEINS

The network of quartz-tourmaline veins related to post-consolidation fractures provides evidence of mul-

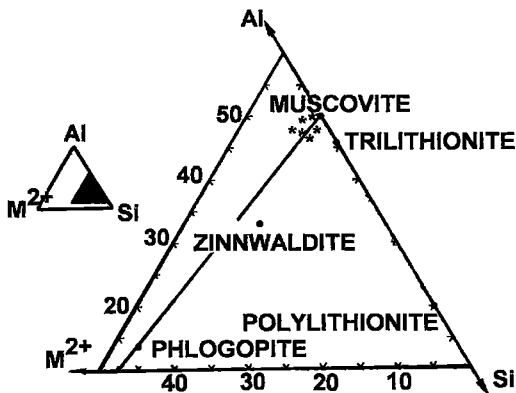


FIG. 3. Composition of muscovite from exogreisen alteration plotted in the Al - M²⁺ - Si diagram.

TABLE 2. CONCENTRATION OF TRACE ELEMENTS IN MUSCOVITE FROM ZONE OF EXO GREISEN ALTERATION

Sample	Ba	Nb	Zr	Sr	Rb	Sn	Y	Zn	Cu	Ni	Pb	Th	V
1	138	36	41	16	610	54	311	61	18	16	41	11	32
2	166	34	67	18	523	61	346	58	12	17	33	8	29
3	312	33	47	29	466	38	338	44	<5	19	38	<5	45
4	136	29	13	<5	512	46	377	56	16	18	64	21	42

Samples 1-3 are light yellowish green muscovite. Sample 4 consists of kaolinitized muscovite. Concentrations are expressed in parts per million.

tle episodes of shearing. Boron- and silica-rich fluid represents the last hydrothermal pulsations generated by processes of differentiation and crystallization of the granitic magma. At the border of the quartz-tourmaline veins, a granophytic facies consists of large flakes (1-2 cm) of muscovite partially altered to kaolinite and K-feldspar phenocrysts fully or partially altered to halloysite-7Å and a Si/Al gel. The last pulse of hydrothermal activity resulted in the K-feldspar crystals accompanying the quartz-tourmaline vein. It seems most probable that K-feldspar here was a metastable phase. The local increase in H activity produced the destabilization of the feldspar structure and generated secondary muscovite associated also with the quartz + tourmaline veins.

TABLE 3. CHEMICAL COMPOSITION OF TOURMALINE FROM SÃO VICENTE DE PEREIRA KAOLIN DEPOSIT

Samples	1	1a	2	3	4	5	6
n*	3	4	3	3	2	4	4
SiO ₂ wt. %	33.77	34.55	36.17	37.63	39.23	39.81	39.16
TiO ₂	1.19	1.16	1.41	0.91	0.59	0.00	0.00
Al ₂ O ₃	29.06	29.86	30.21	33.24	34.94	35.98	34.68
FeO	29.36	28.63	26.90	22.94	20.23	13.45	13.39
MgO	3.48	3.21	2.03	3.00	3.06	6.95	8.17
CaO	1.41	0.85	0.68	0.46	0.66	1.24	1.83
Na ₂ O	1.58	1.42	2.51	1.38	1.26	3.09	2.75
K ₂ O	0.16	0.36	0.09	0.44	0.03	0.03	0.02
S	0.00	0.00	0.00	0.16	0.55	0.00	0.00
Total	100.00	100.00	100.00	100.00	100.00	100.00	100.00

number of cations calculated on the basis of 24.5 atoms of oxygen

	Si	Ti	Al	Fe	Mg	Ca	Na	K
Si <i>apfu</i>	5.39	5.46	5.66	5.72	5.84	5.79	5.72	
Ti	0.14	0.14	0.17	0.10	0.06	0.00	0.00	
Al	5.46	5.57	5.57	5.95	6.13	6.11	5.96	
Fe	3.91	3.79	3.52	2.91	2.52	1.63	1.63	
Mg	0.83	0.75	0.47	0.68	0.68	1.51	1.78	
Ca	0.24	0.14	0.11	0.07	0.10	0.19	0.29	
Na	0.49	0.43	0.76	0.40	0.36	0.87	0.78	
K	0.03	0.07	0.02	0.08	0.00	0.00	0.00	

*n: number of analyses carried out. The compositions are normalized on an anhydrous, boron-free basis. Samples: 1, 1a: tourmaline with a higher oxidation state; 2 and 3: zoned tourmaline (polygonal habit) from quartz veins; 4: tourmaline from veinlets in kaolinite deposit; 5, 6: tourmaline of acicular habit from quartz-tourmaline greisen.

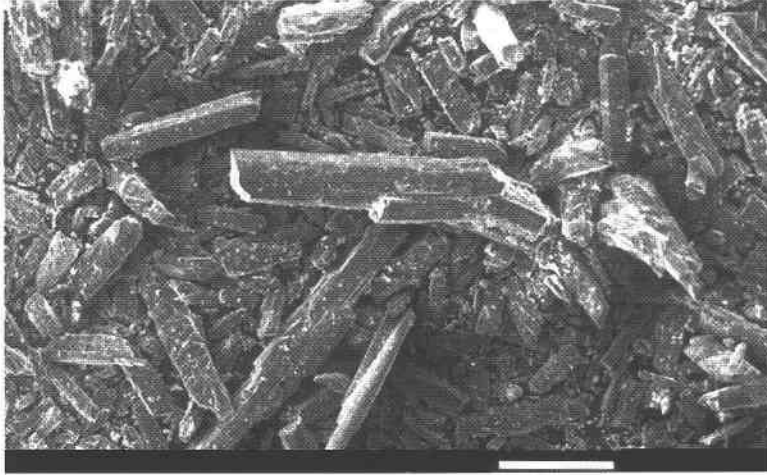


FIG. 4. SEM image of acicular tourmaline. Scale bar: 100 μm .

POST-GREISEN ALTERATION

First stage

The first stage of post-greisen alteration is characterized by the enhancement of H^+ metasomatism, which led to the replacement of minerals from the exogreisen system (quartz–muscovite assemblage) by argillic alteration, to yield neoformed clay minerals (*e.g.*, illite and kaolinite).

SEM images of a fracture surface of the bulk material show the transition from platy mica to illite and, finally, to kaolinite (Bobos & Gomes 1997a). Illite crys-

tals exhibit a lath morphology (Fig. 6a), the bundles of laths being oriented in the same direction. These crystals can be considered to have formed on microfractures or on exfoliation surfaces of mica crystals. Pseudomorphs after mica consist of pseudo-hexagonal platelets of kaolinite associated in "booklet" aggregates (Fig. 6b). Flakes of kaolinite also are found at the edges of the mica packets.

Electron-microprobe analyses show a decrease in K, from 11.32 to 2.56% K_2O , during the transformation mica \rightarrow illite \rightarrow kaolinite (Table 4). In mixed phases (muscovite–kaolinite) analyzed by EDAX, the content of K decreases from 5.2 to 1.7% K_2O . Also, the atomic ratio Si/Al in the plates of kaolinite is greater than one. The low K content is explained by the alteration of muscovite to illite. Also, Mg is absent in mica, and only a small quantity of Fe was identified in the mixed phases mica–kaolinite.

The mechanism of alteration of muscovite to kaolinite *via* illite involves a gain of H_2O or protons (H^+), necessary to form OH groups coordinating the Al. This transition implies a dissolution and precipitation. Structural changes found in mica are very profound, with intermediate phases being produced.

Second stage

The second stage of post-greisen modifications is characterized by advanced argillic alteration. Great quantities of metamorphic fluid mixed with silica-enriched fluid were discharged in the region, and produced the rapid dissolution of K-feldspar. Supporting evidence for its rapid dissolution due to the migration of the acidic front is clearly expressed in field observations and in electron microscopy investigations. The dissolution of K-feldspar produced a gel having a "kaolinitic" compo-

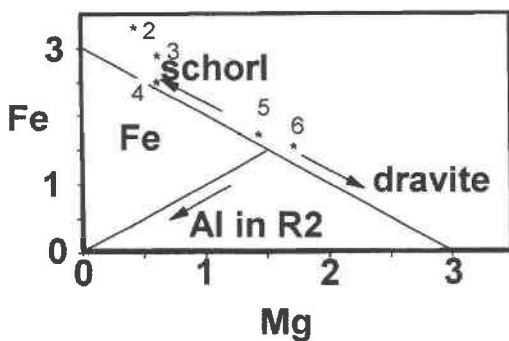


FIG. 5. Plot of Fe versus Mg in atoms per formula unit for tourmalines from São Vicente de Pereira area. Samples 2 and 3 are tourmaline with polygonal habit, sample 4 is tourmaline from dispersed veinlets in the kaolin deposit, and samples 5 and 6 are acicular tourmaline from quartz–tourmaline greisen.

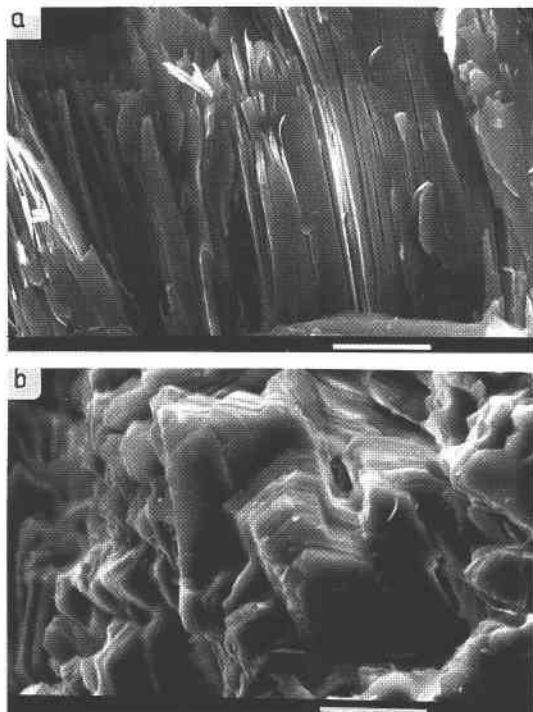


FIG. 6. SEM images showing the morphological transition of mica to illite (a) and kaolinite "booklets" (b). Both minerals were identified in the same grains of altered mica. Scale bar: 10 μm in both cases.

sition, with a Si:Al ratio equal to unity, and then halloysite-7 \AA was formed (Bobos & Gomes, unpubl. data). SEM observations performed on altered K-feldspar grains reveal the presence of etch pits, variable in size. The K-feldspar thus has been dissolved by acidic solutions, and kaolinite formation is not directly related to K-feldspar.

The mica was transformed completely to kaolinite. TEM investigations of the less than 2 μm fractions re-

veal a well-ordered kaolinite [Hinckley index = 1.07; Hinckley (1963)] showing booklet morphology (Fig. 7), which indicates that kaolinite was formed exclusively from muscovite, the precursor mineral (Bobos & Gomes 1997b). Halloysite was not identified as an alteration product of mica.

Chemical analyses of well-ordered kaolinite (Table 5) show an atomic ratio Si:Al ranging from 1.01 to 1.03. No structurally bound iron was identified in the plates of kaolinite.

Weathering processes

Gibbsite, amorphous aluminum hydroxide and phosphates, typical products of the weathering process, were not identified. However, the structural transition from well-ordered kaolinite to halloysite-7 \AA was identified. Along this transition, the Si:Al ratio decreases to values less than unity. The hydration of kaolinite increases as kaolinite transforms to halloysite-7 \AA , and it was one of the main factors responsible for this transformation (Bobos & Gomes 1997b). Some plates of kaolinite are partially rolled and exhibit a lath morphology under TEM investigation.

Field data show that the transition of kaolinite to halloysite-7 \AA took place from the central part of the kaolinite deposit, where quartz \pm tourmaline veins occur, toward the external part of the deposit, close to the contact with the micaceous schist complex.

Also, another generation of halloysite-7 \AA related with a Si-Al gel was identified in the kaolinite deposit.

Oxygen isotope data on kaolinite

The oxygen isotope ratio ($\delta^{18}\text{O}$, in ‰) of well-ordered and moderately ordered kaolinite formed from muscovite, the precursor mineral, has been determined (Table 6). The data were correlated with Hinckley crystallinity index measured on samples of kaolinite. Two values of the deuterium isotope ratio (δD , in ‰) were determined as well. A $\delta^{18}\text{O}$ of 12.1‰ was measured for well-ordered kaolinite, which occur close to quartz veins. According to Taylor (1974) and Sheppard (1981), the presence of metamorphic fluid is characterized by

TABLE 4. CHEMICAL TRANSITION OF MUSCOVITE INTO ILLITE AND KAOLINITE FROM GREISEN AND POST-GREISEN ALTERATION

Samples <i>n</i> *	1	2	3				
	3	3	4	1	2	3	
	3	3	4	3	3	4	
SiO ₂ wt. %	49.92	52.88	52.74	K ₂ O	11.32	6.24	2.56
Al ₂ O ₃	38.08	40.22	41.12	P ₂ O ₅	0.00	0.00	1.37
FeO	0.53	0.25	0.58	SO ₃	0.00	0.00	0.71
CaO	0.00	0.19	0.06	Cl	0.04	0.09	0.02
MgO	0.00	0.00	0.00	Total	100.00	100.00	100.00
Na ₂ O	0.15	0.04	0.42	[Si]/[Al]	1.11	1.12	1.09

*n**: number of analyses. Samples: 1: muscovite, 2: illite, 3: kaolinite. Compositions are normalized to an anhydrous basis.

TABLE 5. CHEMICAL COMPOSITION OF THE LESS THAN 2 μm FRACTIONS OF KAOLINITE

Samples	K ₁	K ₂	K ₃	K ₄	K ₅
Si <i>apfu</i>	1.98	1.99	1.98	1.98	1.99
Al	1.98	1.97	1.96	1.95	1.93
Na	0.01	0.00	0.00	0.01	0.01
K	0.03	0.00	0.03	0.03	0.02
Si/Al	1.01	1.01	1.02	1.02	1.03

K₁ to K₅ are samples of well-ordered kaolinite with a Hinckley index greater than 1.

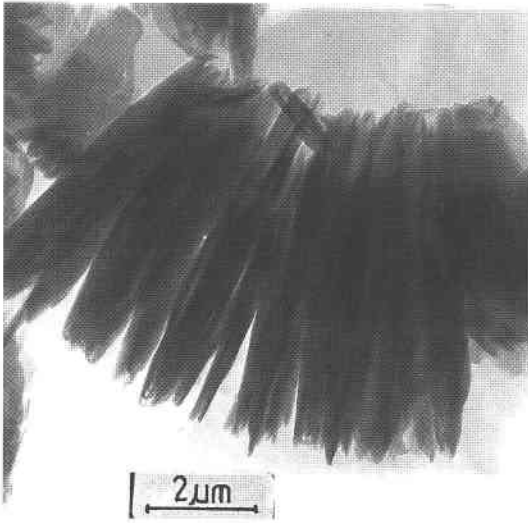


FIG. 7. TEM image showing kaolinite "booklet" identified in the $<2 \mu\text{m}$ clay fraction. All specimens of kaolinite exhibit the same morphology. No individual pseudo-hexagonal crystals of kaolinite were identified.

δD values in the interval -65 to -20‰ , whereas for $\delta^{18}\text{O}$, the values may range in the interval $+3$ to $+25\text{‰}$. The values obtained on kaolinite samples from São Vicente de Pereira area satisfy the above generalizations. The values plot in the "box" expected for metamorphic fluid (Fig. 8). The kaolinite line discriminates kaolinite having hydrothermal or weathering origins (Sheppard *et al.* 1969). To the right of the supergene-hypogene line are plotted kaolinite samples formed as a result of weathering.

Samples of hydrothermal kaolinite related with the Kuroko deposit in Japan (Marumo 1989) and of supergene kaolinite from late Cretaceous and Oligocene deposits at Iwaizumi (Japan), formed by weathering of volcanic parent rocks (Mizota & Longstaffe 1996), also are shown in Figure 8.

DISCUSSION

The kaolinite deposit of São Vicente de Pereira area hosts a quartz-muscovite and quartz-tourmaline exogreisen. An extensive occurrence of quartz-tourmaline veins is found in the Lourosa unit (migmatite complex) accompanying the shear zone. The veins form a network, particularly well developed near the main fracture (Fig. 1).

Evidence of greisenization confirms the postmagmatic alteration of a primary rock (granite) by solutions enriched in volatiles associated with the cooling of the granitic body. However, only sparse information concerning the nature of the fluids responsible for greisen

formation is available. Usually, a greisen system occurs as a succession of different stages of alteration that reflect arrival of solutions at various stages, ranging from magmatic to postmagmatic. Our data cover only the final stages of a greisen system, expressed by a metamorphic greisen (quartz + muscovite bearing F and Cl) formed by decomposition of plagioclase. The quartz-muscovite exogreisen was followed by progressive stages of F- and B-metasomatism. The last hydrothermal pulses were enriched in Si and B, which developed an extensive network of quartz-tourmaline veins along the main fault.

Silicification and tourmaline formation are two postmagmatic processes that accompanied the greisen system at São Vicente de Pereira. Silicification gave rise to the common quartz "flooding" of the greisenized rocks; it took place during and after the greisenization process.

Argillic alteration (mica \rightarrow illite \rightarrow kaolinite) corresponds to the last hydrothermal stage, after the evolution of the greisen system. Quartz-muscovite greisen identified in the kaolinite deposit can be considered as relict alteration, partially conserved in spite of the post-greisen alteration.

Other types of greisen (*e.g.*, quartz-topaz) were not identified in the region. The outcrop area is not extensive, and the depth of exploitation for kaolinite is very shallow.

However, the advanced argillic alteration has a very wide distribution parallel to the fault zone (Fig. 1), which suggests a possible link to the shear zone. Also, in morphological terms, the zone of argillic alteration from the Lourosa unit does not form a mushroom-shaped cap typical for the apical zone of a tin-bearing pluton; instead, it forms a series of steeply dipping tabular zones that are concordant with the foliation of the migmatite zone that defines the shear zone. For the Ossa Morena zone, we postulate a possible intersection of the shear zone with crystallizing intrusions, which generated this symbiotic post-greisen alteration of a greisen system and an advanced argillic alteration hosted in a shear zone. Several cases are reported in the literature where a shear zone is characterized by the development of an intense foliation in mica; usually, the shear zone

TABLE 6. ISOTOPIC DATA FOR KAOLINITE ($K_1 - K_3$) FROM SÃO VICENTE DE PEREIRA

Samples	K_1	K_2	K_3	K_4	K_5
$\delta^{18}\text{O}$	19‰ ± 1.3	17.1‰ ± 0.1	12.4‰ ± 0.1	9.9‰	14.2 to 16.6‰
δD	-62‰	-59‰	ndt	-26 to -28‰	-97 to -103‰

K_1 : kaolinite related to the Kuroko deposit (Marumo 1989); K_2 : kaolinite from the Iwaizumi clay deposit (Mizota & Longstaffe 1996). ndt: not determined.

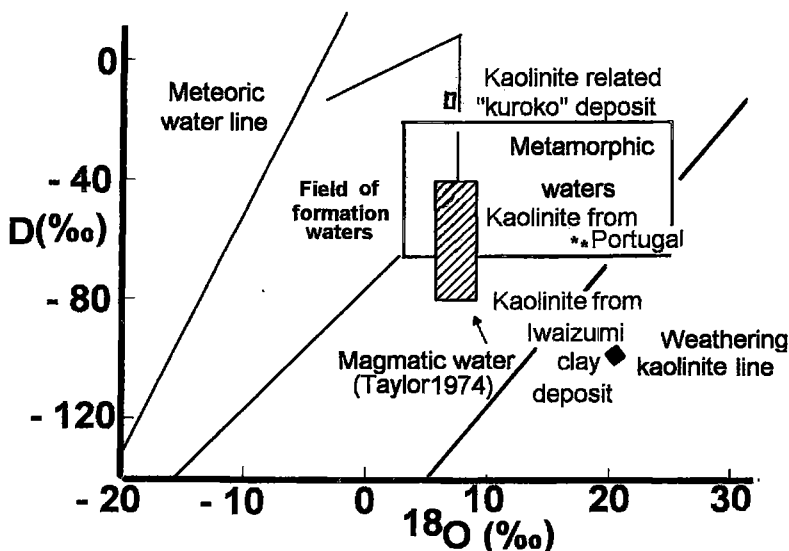


Fig. 8. Plot of $\delta^{18}\text{O}$ (‰) versus δD (‰). The field (*) corresponds to well-ordered kaolinite from the São Vicente de Pereira kaolinite deposit. Other fields corresponding to: hydrothermal kaolinite related to "Kuroko" deposit from Japan (□) and supergene kaolinite from the Cretaceous and Oligocene Iwaizumi clay deposits, Japan (◆).

is coincident with the elongate zone of alteration. Both cases are well documented in the São Vicente de Pereira area and along the migmatite complex.

The process of migmatization played an important role in the formation of the advanced argillic alteration. The H_2O within the shear zone may have been derived from the migmatization process. Fluid flow in shear zones is predicted to be episodic and dominated by transient fracture-induced permeability (McCaig 1988). Various studies have shown that shear zones can provide important conduits for fluid movement through the crust (Beach 1976, McCaig 1988). Unfortunately, this phenomenon is still poorly understood.

In spite of the paucity of data, two episodes of argillic alteration seem to have occurred in the region; one is local, related with the greisen system, and the second, very widespread, is related with the discharge of great quantities of metamorphic fluid into the major shear-zone. As a result of this activity, advanced argillic alteration was produced. Zones of advanced argillic alteration enriched in kaolinite and halloysite-7Å were superimposed on the first stage of argillic alteration.

The geological episodes that did occur in the region, consistent with the Hercynian polyphase deformation (Aguado 1992, Aguado *et al.* 1993, Ribeiro *et al.* 1995), can be summarized as follows:

1. Granitic rocks of the Oliveira de Azemeis pluton (pre- D_3) outcrop in the southern part of the northwestern border of the Ossa Morena zone. The granitic rocks are considered by Aguado (1992) to be contemporary

with post- D_2 deformation. The same type of granitic rock may or may not have been involved in a migmatization process, well developed in the antiform D_3 . The process of migmatization is synchronous with D_3 deformation.

2. Postmagmatic alteration (greisenization) is found in the São Vicente de Pereira area, expressed by an exogreisen; quartz-muscovite and quartz-tourmaline assemblages were formed most probably before or during D_3 deformation; the composition of the hydrothermal fluids is characterized by enhanced activities of H, B, F and Cl, responsible for the breakdown of the primary minerals; a first stage of greisenization may be associated to an endogreisen environment, located most commonly at the top of the granitic cupola.

3. The mica of the greisen exhibits a structural arrangement expressed by crenulations and microfolds, an argument that mica grains supported at least one major regional tectonic deformation (D_3 or D_4 or both).

4. A post-greisenization stage expressed by the sequence muscovite \rightarrow illite \rightarrow kaolinite is associated with advanced argillic alteration, very widespread in the Lourosa unit. Advanced argillic alteration is related with a great discharge of metamorphic fluid produced on a large scale, after the migmatization process.

ACKNOWLEDGEMENTS

I.B. gratefully acknowledges the Praxis XXI BCC/4815 scholarship provided to him by Fundação de

Ciência e Tecnologia – Lisboa. Thanks are due to Prof. Robert F. Martin, to Dr. Prakash Malla and to an anonymous reviewer for constructive reviews. Also, our gratitude goes to Drs. Norbert Clauer and Jean-Pierre Girard for the help provided with the isotope analyses. Dr. Beatriz Valle Aguado provided help in the interpretation of field relationships to the first author.

REFERENCES

- AGUADO, V.B. (1992): *Geología estructural de la Zona de Cizalla de Porto-Tomar en la región de Oliveira de Azeméis – Serra de Arada (Norte de Portugal)*. Tesis Doctoral, Univ. de Salamanca, Salamanca, Spain.
- _____, ARENAS, R. & MARTINEZ CATALAN, J.R. (1993): Evolucion metamorfica hercinica en la region de la Serra de Arada (Norte de Portugal). *Comun. Inst. Geol. e Mineiro-Lisboa* **79**, 41-61.
- BARNES, H.L., ed. (1979): *Geochemistry of Hydrothermal Ore Deposits*. Wiley Interscience, New York, N.Y.
- BEACH, A. (1976): The interrelations of fluid transport, deformation, geochemistry and heat flow in Early Proterozoic shear zones in the Lewisian complex. *R. Soc. London Philos. Trans. A* **280**, 569-604.
- BOBOS, I. & GOMES, C.S.F. (1996): Kaolin deposit of São Vicente de Pereira (Portugal). In Proc. Eurolat'96 (C. Gomes, ed.). *Geociencias (Rev. Univ. de Aveiro, Portugal)* **10**(1), 167-178.
- _____ & _____ (1997a): Pseudomorphs of kaolinite after muscovite: morphological and chemical data. *Golden Jubilee Meeting (Aberdeen), Clay Minerals Group, Abstr. Program*, 6.
- _____ & _____ (1997b): Lath shape kaolinite to halloysite-7Å transition: morphological, structural and chemical data. *Golden Jubilee Meeting (Aberdeen), Clay Minerals Group, Abstr. Program*, 7.
- BRINDLEY G.M. & BROWN, G., eds. (1980): *Crystal Structures of Clay Minerals and their X-Ray Identification*. Mineralogical Society, London, U.K.
- CHAMINÉ, H.I., RIBEIRO, A. & PEREIRA, E. (1995): Cartografia geológica e estratigrafia da faixa precâmblica do sector Espinho – Albergaria-A-Velha (Zona de Ossa-Morena). *Faculdade de Ciências, Universidade do Porto, Memória* **4**, 329-333.
- GIRARD, P.J. & FOULLAC, A.M. (1995): Oxygen and hydrogen isotope geochemistry of clays: examples of application to diagenetic and geothermal environments. *Bull. des Centres de Rech. Explor.- Prod. Elf Aquitaine* **19**(1), 167-195.
- GOMES, C., VELHO, L.G.A.J. & DELGADO, M.H. (1990): Kaolin deposits of Portugal. *Geociencias (Rev. Univ. de Aveiro)* **5**(2), 75-84.
- HINCKLEY, D.N. (1963): Variability in "crystallinity" values among the kaolin deposits of the coastal plain of Georgia and South Carolina. *Clays Clay Mineral.* **11**, 229-235.
- LONDON, D. & MANNING, D.A.C. (1995): Chemical variation and significance of tourmaline from southwest England. *Econ. Geol.* **90**, 495-519.
- MARUMO, K. (1989): Genesis of kaolin and pyrophyllite in Kuroko deposits of Japan: implications for the origins of the hydrothermal fluids from mineralogical and stable isotope data. *Geochim. Cosmochim. Acta* **53**, 2915-2923.
- MCCAIG, A.M. (1988): Deep fluid circulation in fault zones. *Geology* **16**, 867-870.
- MIZOTA, C. & LONGSTAFFE, F.J. (1996): Origin of Cretaceous and Oligocene kaolinities from the Iwaizumi clay deposit, Iwate, northeastern Japan. *Clays Clay Minerals* **44**, 408-416.
- NEIVA, A.M.R. & CAMPOS COSTA, T. (1993): The zoned granitic pluton of Penamacor-Monsanto, central Portugal: hydrothermal alteration. *Mem. e Not., Publ. Mus. Lab. Mineral. Geol., Univ. Coimbra* **116**, 22-47.
- _____, NEIVA, J.M.C. & SILVA, M.M.V.G. (1990): Geochemistry of quartz veins walls from Jales (northern Portugal). *Chem. Geol.* **82**, 217-251.
- PIRAJNO, F. (1992): *Hydrothermal Mineral Deposits*. Springer Verlag, New York, N.Y.
- POLLARD, P.J. (1983): Magmatic to postmagmatic processes in the formation of rocks associated with rare element deposits. *Trans. Inst. Mining Metall.* **92**, B1-B9: 211-223.
- RIBEIRO, A., PEREIRA, E., CHAMINÉ, H.I. & RODRIGES, J. (1995): Tectónica do megadomínio de cisalhamento entre a Zona de Ossa-Morena e a Zona Centro-Ibérica na região de Porto-Lousã. *Faculdade de Ciências – Universidade do Porto, Memoria* **4**, 299-303.
- SHEPPARD, S.M.F. (1981): Stable isotope geochemistry of fluids. In *Chemistry and Geochemistry of Solutions at High Temperatures and Pressures* (D.T. Rickard & F.E. Wickman, eds.). *Phys. Chem. Earth* **13/14**, 419-445.
- _____, NIELSON, R.L. & TAYLOR, H.P., JR. (1969): Oxygen and hydrogen isotope ratios of clay minerals from porphyry copper deposits. *Econ. Geol.* **64**, 755-777.
- ŠTEMPROK, M. (1987): Greisenisation. A review. *Geol. Rundsch.* **76**, 169-175.
- TAYLOR, H.P., JR. (1974): The application of oxygen and hydrogen isotope studies to problems of hydrothermal alteration and ore deposition. *Econ. Geol.* **69**, 843-883.

Received August 15, 1998, revised manuscript accepted January 9, 1999.